Journal of Imaging Science and Technology® 65(6): 060404-1–060404-14, 2021.

Structure-Aware Halftoning Using the Iterative Method Controlling the Dot Placement

Fereshteh Abedini▲ and Sasan Gooran
Linköping University, Media and Information Technology Division, Department of Science and Technology, Norra Grysgatan 10, Norrköping, 60233, Sweden
E-mail: fereshteh.abedini@liu.se

Vlado Kitanovski▲
Norwegian University of Science and Technology, Faculty of Information Technology and Electrical Engineering, Department of Computer Science, Teknologiveien 22, Gjøvik, 2815, Norway

Daniel Nyström
Linköping University, Media and Information Technology Division, Department of Science and Technology, Norra Grysgatan 10, Norrköping, 60233, Sweden

Abstract. *Many image reproduction devices, such as printers, are limited to only a few numbers of printing inks. Halftoning, which is the process to convert a continuous-tone image into a binary one, is, therefore, an essential part of printing. An iterative halftoning method, called Iterative Halftoning Method Controlling the Dot Placement (IMCDP), which has already been studied by research scholars, generally results in halftones of good quality. In this paper, we propose a structure-based alternative to this algorithm that improves the halftone image quality in terms of sharpness, structural similarity, and tone preservation. By employing appropriate symmetrical and non-symmetrical Gaussian filters inside the proposed halftoning method, it is possible to adaptively change the degree of sharpening in different parts of the continuous-tone image. This is done by identifying a dominant line in the neighborhood of each pixel in the original image, utilizing the Hough Transform, and aligning the dots along the dominant line. The objective and subjective quality assessments verify that the proposed structure-based method not only results in sharper halftones, giving more three-dimensional impression, but also improves the structural similarity and tone preservation. The adaptive nature of the proposed halftoning method makes it an appropriate algorithm to be further developed to a 3D halftoning method, which could be adapted to different parts of a 3D object by exploiting both the structure of the images being mapped and the 3D geometrical structure of the underlying printed surface.*

[DOI: 10.2352/J.ImagingSci.Technol.2021.65.6.060404]

1. INTRODUCTION

Digital halftoning is a technique to convert a continuous-tone image into a binary image in the image reproduction workflow for printing purposes. The key idea of halftoning algorithms is based on the fact that the human visual system (HVS) functions as a low-pass filter [1]. Most halftoning methods reproduce the image by optimally placing dots such that the quantization error is shifted to higher frequencies—that are hardly perceptible. Halftoning algorithms are usually divided into three main categories: thresholding and table halftoning [1], error diffusion [2–6], and iterative [7–10] methods. Thresholding and non-modified error diffusion are simple techniques, but they introduce different types of artifacts and worsen the representation of the original image. However, iterative methods such as the Direct Binary Search (DBS) [7] and the Iterative Method Controlling the Dot Placement (IMCDP) [8] generate higher quality halftones at the cost of computational complexity.

A high-quality halftone should present tonal and structural resemblance to the original image. However, it is possible that important structural details, such as edges, are smoothed in the halftoning process. Because the edges are an important consideration in human perception [11], some halftoning algorithms fail to truly convey the appearance of the original image. In order to improve the quality of halftone reproduction, many researchers have developed structure-based halftoning algorithms on the basis of the classical halftoning techniques [11–19]. The main idea of structure-based halftoning algorithms is to employ the important information derived from the original image content, such that the halftone better resembles the original image.

In this study, we leverage the possibility of creating different halftone structures, using the IMCDP [8], and detecting the orientation of local lines by the Hough Transform [20] to develop a line-based IMCDP. The main goal is to enhance the edge reproduction compared to the classical IMCDP through the halftoning process. Thus, the reproduction of the image structure improves, and the halftone better represents the fine details and structural features of the original image. The challenge is to find a balance between the degree of sharpness enhancement and the increase in tonal and structural similarity. Besides

▲ IS&T Members.

Received July 28, 2021; accepted for publication Oct. 26, 2021; published online Nov. 17, 2021. Associate Editor: Johoon Kim.

1062-3701/2021/65(6)/060404/14/$25.00

improving the quality of 2D-halftone images, another benefit of the proposed line-based method is that it can be extended to an adaptive structure-based 3D halftoning method. It can be adapted to different parts of a 3D object by exploiting the structure of the image being mapped and the 3D geometrical structure of the underlying printed surface.

2. RELATED WORK

Digital halftoning has been studied for many years with the aim of using a limited number of inks to reproduce an image that resembles the original image [1]. The improvements on halftoning quality have focused on reducing visible artifacts, increasing tone consistency, and better preserving the structures of the original image.

Thresholding and table-halftoning techniques are point-process algorithms with simple calculations but produces undesirable artifacts. Error diffusion, which was first proposed by Floyd and Steinberg [2], is considered as a neighborhood-process algorithm with higher reproduction quality than thresholding and table halftoning. Eschbach and Knox improved the edge reproduction in the error diffusion algorithm by introducing the inverse of the input image as a threshold into the halftoning process [12]. Later, Ostromoukhov distributed the error diffusion's coefficients over different intensity levels through an offline process [3]. Zhou and Fang focused on reducing the mid-tone visual artifacts and proposed a variable threshold modulation for the error diffusion algorithm [4]. Li and Allebach optimized the filter weights and thresholds in error diffusion based on a human visual model and proposed a tone-dependent error diffusion. Their modifications removed most of the visual artifacts generated by non-modified error diffusion algorithms [21]. Li and Mould extended the Floyd–Steinberg error diffusion to improve tone and structure similarity [11]. They focused on preserving the local contrast by using an adaptive contrast-aware mask. However, they have reported that the black pixels are not optimally placed. Moreover, they have not discussed whether a higher contrast always results in a more pleasant structure. Pang et al. proposed a structure-aware halftoning algorithm, which optimizes an objective function consisting of structure and tone metrics [13]. Chang et al. used the local frequency content of the original image and improved the visual quality of the error diffusion [14]. They proposed a method that generates halftones with visual quality comparable to those presented by Pang et al., but it is much faster. Liu et al. proposed an entropy-constrained modulation that improves the error diffusion algorithm in preserving the structure and tone similarity [15]. Recently, Li et al. proposed a texture-aware multi-level error diffusion halftoning to better represent the texture of images [16].

Iterative halftoning algorithms such as the DBS [7] and IMCDP [8] methods generate halftones with higher quality than error diffusion at the cost of computational complexity. Baqai and Allebach enhanced detail reproduction and tone preservation in the DBS algorithm by considering the printer model in the halftoning process [22]. In this study, we aim to improve the IMCDP halftoning algorithm by enhancing the edge reproduction while preserving the tonal and structural content of the original image.

3. METHOD

In this section, we describe our proposed method to enhance the reproduction of structural details through halftoning. The proposed method is based on the IMCDP halftoning algorithm [8] and the Hough Transform [20]. The goal is to improve the structure of the details in the halftone while preserving the tonal and structural resemblance to the original image. The key idea of our proposed method is to modify the dot placement and align the halftone structure with the high-frequency details of the image. Before describing the proposed algorithm, we briefly introduce the IMCDP and Hough Transform methods.

3.1 *IMCDP*

The classical IMCDP starts with a blank image of the same size as the original continuous-tone image. The algorithm searches over the whole original image for the pixel holding the maximum value; then, a “1” or a black dot is placed at its corresponding position in the blank image. To ensure that this position will not be selected as the maximum pixel again, a very small value is set to this position in the original image. Then, to consider the effect of this quantization, the low-pass filtered version of the halftone image is subtracted from the low-pass filtered version of the original image. This low-pass filter in IMCDP, called the feedback filter, is a symmetrical Gaussian filter with a standard deviation of σ, which is defined as:

$$f(x, y) = Ke^{-((x^2+y^2)/2\sigma^2)}. \tag{1}$$

In Eq. (1), K is a normalization factor to ensure that the filter elements sum into 1, and (x, y) is the position of each pixel.

Applying the filter reduces the probability of finding the next maximum in the neighborhood of the same pixel in the next search. The algorithm continues by finding the pixel with the second highest value in the next iteration. As the average intensity value over every tonal region should remain the same in the original and halftone image, the total number of black dots to be placed in different regions of the halftone image is known in advance. Therefore, the algorithm continues until the predetermined number of black dots is placed and the halftone image is created [8].

The Gaussian filter in Eq. (1) is a symmetrical filter, so the halftone dots are placed symmetrically in all directions. However, a non-symmetrical Gaussian filter can produce halftones with different structures and alignments [23].

Thus, modifying the Gaussian kernel in Eq. (1) to create a non-symmetrical Gaussian filter as:

$$f(x, y) = Ke^{-(Ax^2+2Bxy+Cy^2)}. \tag{2}$$

In Eq. (2), K is a normalization factor to ensure that the filter elements sum into 1 and the constants A, B, and C are calculated as:

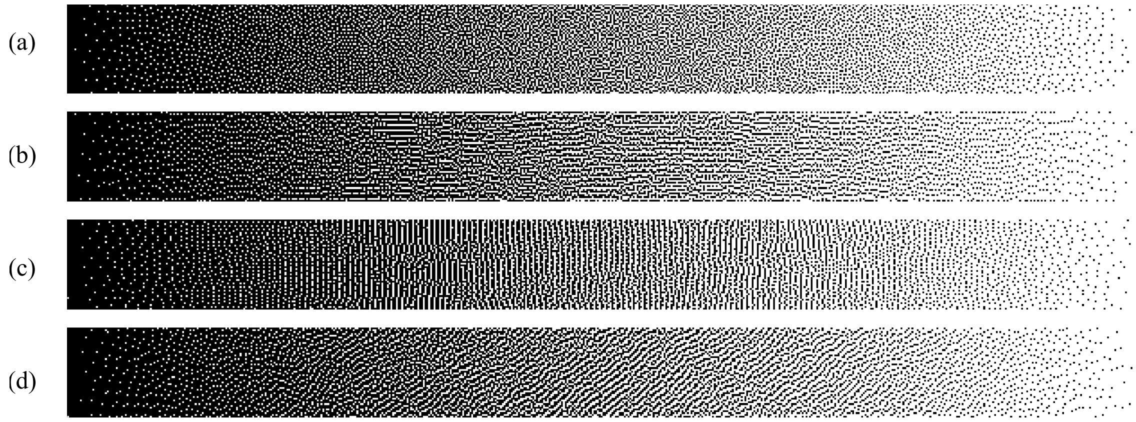

Figure 1. Grayscale ramp being halftoned by the IMCDP algorithm. (a) Using the symmetrical filter in Eq. (1), (b) using the non-symmetrical filter in Eq. (2) with horizontal alignment $k_1 = 1$, $k_2 = 3$, $\varphi = 0°$, (c) using the non-symmetrical filter in Eq. (2) with vertical alignment $k_1 = 3$, $k_2 = 1$, $\varphi = 0°$, (d) using the non-symmetrical filter in Eq. (2) with horizontal alignment $k_1 = 1$, $k_2 = 3$, rotated by $\varphi = 30°$. Halftone ramps are displayed at 100 dpi. This figure is best viewed in the electronic version of this paper.

$$A = \frac{\cos^2\varphi}{2k_1\sigma^2} + \frac{\sin^2\varphi}{2k_2\sigma^2}, \tag{3}$$

$$B = \frac{-\sin 2\varphi}{4k_1\sigma^2} + \frac{\sin 2\varphi}{4k_2\sigma^2}, \tag{4}$$

$$C = \frac{\sin^2\varphi}{2k_1\sigma^2} + \frac{\cos^2\varphi}{2k_2\sigma^2}. \tag{5}$$

The Gaussian function presented in Eq. (2), has a non-symmetrical (elliptical) kernel. The parameters k_1 and k_2 could be used to adjust the symmetry of the Gaussian filter. Setting $k_1 = k_2$ creates halftones similar to the classical IMCDP. While $k_1 > k_2$ makes halftones grow faster in the vertical direction, conversely, $k_1 < k_2$ generates halftones with horizontal alignments. Using Eq. (2) generates halftones with line structures, referred to as line halftone structure throughout this paper. The angle φ specifies the direction of dots' placement with regards to the positive x-axis.

For creating a halftone structure in different directions, it is possible to generate the halftone in one direction and then adjust its direction by changing the angle φ. This simply means that the halftone structure could be rotated by the desired angle φ. By setting $k_1 = k_2 = 1$, Eq. (2) forms a symmetrical Gaussian filter equal to the one presented in Eq. (1).

Figure 1 illustrates a grayscale ramp being halftoned with symmetrical and non-symmetrical Gaussian filters using Eqs. (1) and (2), respectively. As can be seen in this figure, the IMCDP reproduces well-formed halftone while it enables the user to generate halftones with different structures and alignments.

Furthermore, it was shown that different halftone structures, produced by the IMCDP, could be combined in the same image with smooth transition [24]. The flexibility of the IMCDP in generating line halftone structures makes it a powerful algorithm to develop a method that adaptively changes the halftone structure and alignment based on the content and local structure of the original image.

3.2 *Hough Transform*

The classical Hough Transform has been invented by Hough to detect lines in images [20]. A Canny edge detector is applied to the original image to find pixels lying on the edges [25]. The Canny edge detector results in a binary image, which identifies the pixels that contain the edge information. The idea of the Hough Transform is that, in a 2D space and for each edge point, all candidate lines that could pass through that point are found. For each line, a perpendicular line that intersects the origin is defined. Since the perpendicular line passes through the origin, it can be presented by its angle with the positive x-axis (θ) and its length (ρ). Therefore, the two parameters length and angle of the perpendicular line are an alternative way to parameterize each line passing through the edge points. Indeed, in the neighborhood of each edge point, pixels lying on a shared line result in the same θ and ρ. Every time that an edge point yields the same pair of θ and ρ, a counter is increased for that pair. Hence, the pair which has the largest counter value indicates the dominant line in the corresponding neighborhood. The algorithm then proceeds with the next neighborhood.

Noisy edge detection or noisy points in the original image often result in detecting lines that are not perfectly straight and may contain discontinuity. This problem could be tackled by grouping the potential discontinued lines for each edge point and identifying a perfectly straight line.

The idea of presenting lines by the length and angle of their corresponding perpendicular line enables the user not only to detect lines but also to compute the angle of each line. This makes the Hough Transform an important method for feature extraction in image analysis.

3.3 *Proposed Line-based IMCDP Algorithm*

In this subsection, we introduce the proposed line-based halftoning algorithm. The premise is to develop a halftoning algorithm that adaptively changes the halftone structure based on the image content to better reproduce the structural appearance of the original image. We leverage the possibility of generating line halftones with different alignments using the IMCDP and computing the angle of detected lines in the original image using the Hough Transform to modify the classical IMCDP and propose a line-based IMCDP.

To achieve our objective, the task is divided into two phases: preprocessing and halftoning. In preprocessing, the dominant line in the neighborhood of each pixel is identified and the input image is partitioned into structureless and structured regions. In the halftoning phase, different forms of Gaussian filters are used based on the alignment of the dominant line. To be more specific, in the neighborhood of the pixels that lie in the structureless regions a symmetrical Gaussian filter (as defined in Eq. (1)) is used in the feedback process, while in the neighborhood of the pixels that are in the structured regions a non-symmetrical filter (as defined in Eq. (2)) is used. Sections 3.3.1 and 3.3.2 elaborate on the two phases of the proposed algorithm.

3.3.1 *Preprocessing*

In the pre-processing step, the aim is to extract regions containing important edge information. As structural information plays an important role in representing the appearance of an image, improving the generation of high-frequency components enhances the quality of image reproduction. Thus, to extract high-frequency information of an image, the standard Hough Transform is applied to detect lines in the input image. For each pixel, if any line is detected within its neighborhood of size $N \times N$ pixels, we consider that pixel belonging to a structured region of the image. Otherwise, the pixel lacks structural information in its neighborhood and is categorized as a structureless area of the image. Since the largest feedback filter used in the halftoning algorithm is 21×21 pixels, we found $N = 21$ pixels an effective neighborhood size to detect lines.

Figure 2 illustrates an example of how the Hough Transform is employed to calculate the line's orientation. The detected line and its corresponding perpendicular line are shown in solid and dashed line, respectively. The Hough Transform identifies the detected line using the length of the perpendicular line (ρ) and its angle with the positive x-axis (θ). However, as described in Section 3.1, we are interested in the angle of the detected line with regards to the positive x-axis (φ), which is simply calculated as $\varphi = 90 + \theta$. (For the case illustrated in Fig. 2.)

The Hough Transform detects all the existing lines in a neighborhood, while for every pixel of the image only one line must be selected as the dominant line in its neighborhood. Therefore, we set a threshold of $T = N/2$ to ignore the lines shorter than half of the size of the processed neighborhood; however, there might still be multiple lines detected in a pixel's neighborhood. As the human vision is more sensitive to the horizontal and vertical directions than diagonal ones [26], we select the line which is closer to horizontal (φ close to 0° or 180°) or vertical (φ close to 90°) alignment as the dominant line in each pixel's neighborhood. If more than one line fulfills the criteria for the dominant line,

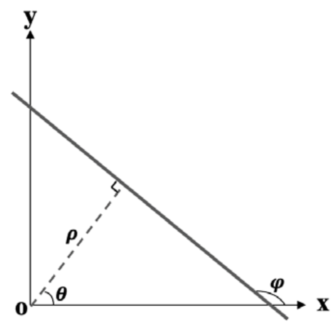

Figure 2. Identifying lines by the Hough Transform. The detected line, in solid, has an angle of φ with the positive x-axis, and its corresponding perpendicular line, in dashed, has a length of ρ and an angle of θ with the positive x-axis.

one of them is arbitrarily selected as the dominant line. Then, the angle of the dominant line (φ) is assigned as a label to the pixel. Pixels with no lines in their neighborhood receive a null label.

The performance of the algorithm has also been evaluated using other criteria for selecting the dominant line and different thresholds. For instance, the longest line was selected as the dominant one, however, the performance of the proposed method is not much affected by this parameter. We determined that $T = N/2$ works well for most images. Section 3.3.2 describes how halftone structures are aligned with image details using the assigned angle to each pixel. The pre-processing step is done independently and before the halftoning process. Thus, the execution time will not affect the process time for halftoning.

3.3.2 *Halftoning*

In the pre-processing phase, by employing the Hough Transform, the input image is partitioned into structured (the union of pixels with lines in their neighborhood) and non-structured (the union of pixels with no line in their neighborhood) regions. Moreover, the Hough Transform provides information about the orientation of the detected lines.

The extracted information in the pre-processing step is used to apply different halftone structures at each pixel. At pixels lying in the structureless region, a symmetrical Gaussian filter, as defined in Eq. (1), is used as the feedback filter while at pixels with a line in their neighborhood the non-symmetrical Gaussian filter, as defined in Eq. (2), is applied as the feedback filter, where the parameter φ is set to the angle of the dominant line in the neighborhood of the under-operation pixel.

As we employ the Hough Transform to compute the angle between the line and the positive x-axis, a horizontal line halftone is created by setting $k_1 < k_2$ in Eq. (2) and then the filter is rotated counterclockwise by the angle φ. As a result, the halftone structure will be aligned with the dominant line in the pixel's neighborhood. Therefore, the edge information is more emphasized, and the halftone image preserves more details at edges.

In the proposed line-based IMCDP, parameters k_1 and k_2 play an important role in the reproduction of high-frequency details of the halftone image; thus, they should be set carefully. On the one hand, the difference between k_1 and k_2 should be large enough to form line halftone structures and enhance edge information, and on the other hand, it should not be so large such that the transition between halftone structures created by different symmetrical and non-symmetrical Gaussian filters would remain smooth. Our approach to investigate the role of k_1 and k_2 in the performance of the proposed algorithm includes both objective and subjective evaluation methods, which are described in Section 3.4.

3.4 *Evaluation Approach*

We study the impact of parameters k_1 and k_2 on the performance of the proposed algorithm through objective and subjective tests. A good halftoning method should generate images with strong edges and preserve tonal information and the structural characteristics of the original image faithfully. In our objective approach, the focus is on measuring the impact of k_1 and k_2 on the following three metrics: sharpness, structural similarity, and tone preservation.

3.4.1 *Perceptual Aspects*

To make a reliable objective evaluation of the halftoning algorithms, it is important to consider the characteristics of the human visual system (HVS)—which creates an illusion of a continuous-tone image when viewing a binary halftone from a suitable distance. The inputs to the three objective metrics are the original continuous-tone image and the halftone output that both need to be simulated using a contrast sensitivity model of the HVS. It was shown that the contrast sensitivity of the HVS could be well modelled by a low-pass filter [1, 26–28]. In this work, we employ a Gaussian function to model the contrast sensitivity filter, as suggested by Pappas and Neuhoff [26]. The standard deviation of the Gaussian kernel depends on the viewing conditions and is calculated as [26]:

$$\sigma = 0.0095 \frac{\pi RD}{180} \text{ pixels.} \tag{6}$$

In Eq. (6), R defines the resolution in *dpi* or *ppi* and D is the viewing distance in inches.

To simulate a printed halftone, we consider the resolution of a typical high-quality printer, 600 *dpi*, and 13 inches viewing distance (33 cm). According to Eq. (6), processing the halftone output with a Gaussian kernel with standard deviation of 1.3 pixels could well simulate the printed halftone. This Gaussian kernel, similarly, simulates a printed halftone at 200 *dpi* resolution being viewed from a 39 inches distance (99 cm).

To evaluate the proposed halftoning algorithm, the original continuous-tone image should also be processed by a Gaussian filter that models the contrast sensitivity of our visual system. To simulate the continuous-tone image, being viewed at a typical display of 100 *ppi* from a 11.8 inches distance (30 cm), we process the original continuous-tone image with a Gaussian kernel with standard deviation of 0.19 pixels (according to Eq. (6)).

Since the halftone and the continuous-tone image are reproduced at different resolutions, two different Gaussian kernels should be applied to properly simulate the contrast sensitivity of the HVS. In all the evaluations in this paper, to account for the contrast sensitivity of the HVS, the halftone and the original image have been processed by the corresponding Gaussian filters before we conduct the measurements.

3.4.2 *Sharpness Metric*

Preservation of details is a critical issue in image reproduction. However, the details of the structural information of the image are often smoothed, especially at the edges, in the halftoning process. Thus, many halftoning algorithms fail in representation of the structural features of the original image [15]. To enhance the high-frequency contents, the halftoning algorithm should be improved to produce sharper images with stronger edges.

There are many techniques to measure sharpness, and for our study, we find the no-reference perceptual blur metric proposed by Crete et al. [29] practical. The key idea of this blur metric is to blur the input image in vertical and horizontal directions. Then, the variation in the neighboring pixels is studied by calculating the absolute difference between the original image and its blurred version. If the variation is high, the input image is sharp, conversely, a low variation shows that the image was already blurred [29]. This metric was developed independent of any edge detector and according to the human perception of sharpness [29]. Furthermore, a subjective evaluation by Crete et al. has shown that the subjective tests correlated with the objective assessment; thus, we find this metric reliable for our objective assessments. The final blur metric value is in the range of 0 to 1 which corresponds to the sharpest and blurriest perception, respectively. Since the blur effect is caused by loss of the high-frequency content, in our evaluations, a low blur metric value is considered as an approximation of greater emphasis on reproduction of high-frequency details in a halftone image.

3.4.3 *Structure Similarity Metric*

Creating sharper halftones and enhancing the reproduction of high-frequency details does not necessarily preserve the texture and structure of the original image. One fundamental requirement, which must be fulfilled through the halftoning process, is to preserve the structural information of the original image. Enhancement in structure reproduction should not be made at the cost of loss or distortion of the original appearance. The aim is to sharpen the halftone image in an efficient way such that no extra structure is introduced to the halftone output. The halftone image should appear visually similar to the original (input) image being viewed from an appropriate distance.

The structural similarity index measure (SSIM) has been proposed by Wang et al. to evaluate the structural similarity between images [30]. SSIM aggregates three terms: luminance, contrast, and structure similarities by a simple multiplication, yielding a similarity evaluation metric defined as:

$$\mathrm{SSIM} = \frac{(2\mu_x\mu_y + c_1)(2\sigma_{xy} + c_2)}{(\mu_x^2 + \mu_y^2 + c_1)(\sigma_x^2 + \sigma_y^2 + c_2)}. \tag{7}$$

In Eq. (7), μ_x and μ_y denote the weighted mean intensity in two images x and y, respectively. Parameters σ_x, σ_y, and σ_{xy} define the standard deviations and the cross-covariance of the two images x and y, respectively. Parameters c_1 and c_2 are small constants to avoid singularity.

In this work, we utilize the mean SSIM (MSSIM) for evaluating the structural similarity of results. MSSIM is the mean value of SSIMs that is computed over blocks of size $L \times L$, and then it quantifies the similarity between the halftone output and the original image by taking average over all pixels. The valid range for the MSSIM is from 0 to 1, a higher value corresponds to a higher similarity. In this work, we set the size of the blocks to $L = 11$.

3.4.4 *Tone Preservation Metric*

Emphasizing the edges and improving the structural similarity without retaining the tonal information of the original image is not acceptable. Retaining tone consistency is also a critical issue in halftoning. However, in the formulated SSIM in Eq. (7), the luminance term is modulated by the contrast and structure components; therefore, SSIM cannot justify the tone similarity [13].

Thus, to effectively measure the tonal fidelity of the proposed line-based IMCDP, we employ the Mean Squared Error (MSE) objective metric, which was used as a tool to measure the tone similarity in related previous work [13]. The MSE quantifies the difference between two images by calculating the second moment of the error. We calculate the MSE values for the images using:

$$\mathrm{MSE} = \frac{1}{M}\sum (I_i - I_h)^2. \tag{8}$$

In Eq. (8), M denotes the total number of the pixels in an image. I_i and I_h are the original and halftone image, respectively, processed by the contrast sensitivity model as described in Section 3.4.1. A smaller MSE accounts for higher tone similarity between the generated halftone and the original image.

3.4.5 *Subjective Test*

To verify the objective approach, we conducted a subjective experiment. In the subjective test, observers are asked to compare the images created by the classical IMCDP and the proposed line-based IMCDP to the original image and evaluate their resemblance to the original image in terms of details and objects' structure.

The test image set includes eight images with different characteristics. Five of them (*Portrait*, *Road*, *Cat*, *Mole*, and *Lion*) are some of the common images which have been used by other researchers to assess their proposed structure-based halftoning algorithms [11]. We used these images to be consistent with the previous works proposed in the literature. The other three images (*Girl* [31], *Flower* [32], and *Relief* [33]) are taken from creativecommons.org website. The *Girl* and *Flower* are images of oil paintings. These two images were added to the test image set because we were interested in evaluating the reproduction of the visible texture of canvas and brushstrokes. The *Relief* is an image of a relief for the chapel which demonstrates a sculpted relief with a high level of details and 2.5D structure. We find this image interesting to test the performance of the proposed halftoning algorithm in displaying three-dimensional feeling and conveying the internal structural features of the image.

Ten observers with normal vision and an average age of 33 participated in the experiment. Only one of the observers was an expert in the field and was from the same lab, and nine of them worked in different fields. In each trial, three images were displayed side by side: The original continuous-tone image was displayed in the middle and the classical IMCDP and the line-based IMCDP were placed either to the left or to the right side of the original image. In total, each observer viewed 96 different trials, considering 8 test images, being halftoned by setting $k_1 = 1$ and 6 different values for k_2 (1.2, 1.4, 1.6, 1.8, 2, 2.2), being displayed on both left and right sides of the original image. The classical IMCDP and the line-based IMCDP images were randomized regarding their position on the display, meaning that they appeared randomly to the left and right side of the original image. The order of displaying the trials for each observer was also randomized.

Each observer was asked to evaluate the two images to the left and right side of the original image (in the middle) and answer one question: "Which image better resembles the image in the middle in terms of details and objects' structure". We provided three options for the answer: "Left", "Right", and "I do not see a difference".

The images were displayed on a screen of size 30 inches with a resolution of 140 *ppi*. The viewing distance was set to 60 cm. The images were processed by the human perceptual model, as described in Section 3.4.1. The observers evaluated the images in a dimmed room such that the display had the highest luminance in the room.

4. RESULTS AND DISCUSSION

In this section, we study the impact of parameters k_1 and k_2 on the performance of the proposed line-based IMCDP. The results produced by the proposed line-based IMCDP are compared to those of the classical IMCDP using both objective and subjective measurements. The proposed algorithm and objective evaluations are implemented using Matlab.

4.1 *Objective Evaluation Results*

We are mainly interested in improving sharpness, structural similarity, and tonal similarity. Hence, the focus is on

Table I. Sharpness evaluation according to blur metric.

Image		Girl	Flower	Relief	Portrait	Road	Cat	Mole	Lion
Classical IMCDP		0.3752	0.4252	0.4415	0.4056	0.3781	0.3731	0.3965	0.3710
Line-based IMCDP	$k_1 = 1, k_2 = 1.2$	0.3639	0.4126	0.4251	0.3896	0.3655	0.3602	0.3841	0.3667
	$k_1 = 1, k_2 = 1.4$	0.3475	0.3925	0.4042	0.3713	0.3507	0.3420	0.3666	0.3580
	$k_1 = 1, k_2 = 1.6$	0.3317	0.3700	0.3812	0.3519	0.3334	0.3234	0.3479	0.3486
	$k_1 = 1, k_2 = 1.8$	0.3158	0.3512	0.3598	0.3378	0.3192	0.3081	0.3296	0.3390
	$k_1 = 1, k_2 = 2$	0.3021	0.3332	0.3394	0.3251	0.3076	0.2949	0.3168	0.3300
	$k_1 = 1, k_2 = 2.2$	***0.2913***	***0.3207***	***0.3256***	***0.3163***	***0.2992***	***0.2840***	***0.3056***	***0.3222***

quantitatively measuring the impact of k_1 and k_2 on three objective evaluation metrics: sharpness, MSSIM and MSE, as described in Sections 3.4.2 to 3.4.4.

4.1.1 *Sharpness*

To investigate the impact of parameters k_1 and k_2 on reproducing sharper halftones, in Eq. (2), we set k_1 to 1 and gradually increase k_2 and calculate the blur metric according to Section 3.4.2. Table I summarizes the blur metric results for the eight test images. As mentioned in Section 3.4.2, the blur metric outputs a value in the range of [0, 1]. Lower values correspond to sharper images.

Comparing the sharpness values in Table I shows that, as expected, images that have been halftoned by the proposed line-based IMCDP result in sharper halftones. That means, the line-based IMCDP performs better than the classical IMCDP in reproducing the details and edge information of the original image. In addition, (according to Table I) by increasing the ratio k_2/k_1, the degree of sharpness improvement increases, which indicates that the degree of sharpness enhancement could be controlled.

Figure 3 illustrates the sharpness improvement by the line-based IMCDP. As can be seen in this figure, the image that is halftoned by $k_2/k_1 = 1.2$ is perceived to be sharper than the image halftoned by the classical IMCDP. Increasing the ratio k_2/k_1 to 1.6 increases the degree of sharpness improvement; so, the halftone in Fig. 3(d) is perceived to be sharper when compared to Fig. 3(c). Visual comparison of the images in Fig. 3 indicates that the line-based IMCDP, specifically, performs better than the classical IMCDP in reproducing the wrinkles under the eye and on the forehead. To ensure that the individual dots and the halftone structure are clearly visible, we demonstrate cropped regions of the halftoned images of Fig. 3. in Figure 4.

4.1.2 *Structural Similarity*

Line-based IMCDP emphasizes the edge information and produces a sharper halftone image. However, it is important to avoid over-emphasizing the high-frequency details and potentially introducing false structure. The halftone structure should resemble the structure of the original image. To assess the performance of the proposed method in preserving the structural similarity, we employ the MSSIM and repeat the same experiment as in Section 4.1.1. Parameter k_1 is set to 1 and k_2 is gradually increased. Table II lists the result for MSSIM. As can be seen in Table II, generally, increasing the ratio k_2/k_1 improves the MSSIM value, but for some images the improvement decreases for larger ratios. For instance, for the image *Girl*, the best MSSIM value corresponds to $k_2/k_1 = 1.6$ and for larger values, the MSSIM value decreases. For *Flower*, *Relief*, and *Mole* the highest MSSIM value is obtained when the ratio k_2/k_1 reaches 1.4, 2, and 1.2, respectively. However, increasing the ratio k_2/k_1 always improves the MSSIM value for *Road*.

4.1.3 *Tone Similarity*

In Section 4.1.1, it was shown that increasing the ratio k_2/k_1 always enhances the degree of sharpness improvement, however, according to our experiments, it does not necessarily result in higher MSSIM. Moreover, as discussed in Section 3.4.4, MSSIM cannot directly account for the tone similarity. Thus, we employ MSE, as a similarity metric, which provides a more reliable tone preservation assessment than MSSIM.

To investigate the impact of parameters k_1 and k_2 on MSE, we set $k_1 = 1$ and gradually increase k_2 (in Eq. (2)) and calculate the MSE value using Eq. (8). Table III summarizes the results for MSE values. As MSE depends on the image intensity scaling, in order to have a true interpretation of the values listed in Table III, it is worth noting that I_i and I_h (in Eq. (8)) are 8-bit images with pixel values in the range from 0 to 255, which means that the largest possible error is 255^2.

According to Table III, generally, the line-based IMCDP results in lower MSE values than the classical IMCDP, indicating that it performs better than the classical IMCDP in preserving the local tone. As can be seen in this table, the best performance on MSE is achieved at $k_2/k_1 = 1.6$ or $k_2/k_1 = 1.8$. Setting the ratio k_2/k_1 to values smaller than 1.6 or greater than 1.8, increases the MSE. This indicates that the tonal information of the original image is not preserved as well as when $k_2/k_1 = 1.6$ or 1.8. In other words, attempts to create sharper halftones do not always result in an improvement in MSE.

Figure 5 summarizes the results of our experiments. The best MSE (i.e., the minimum MSE value) is obtained when

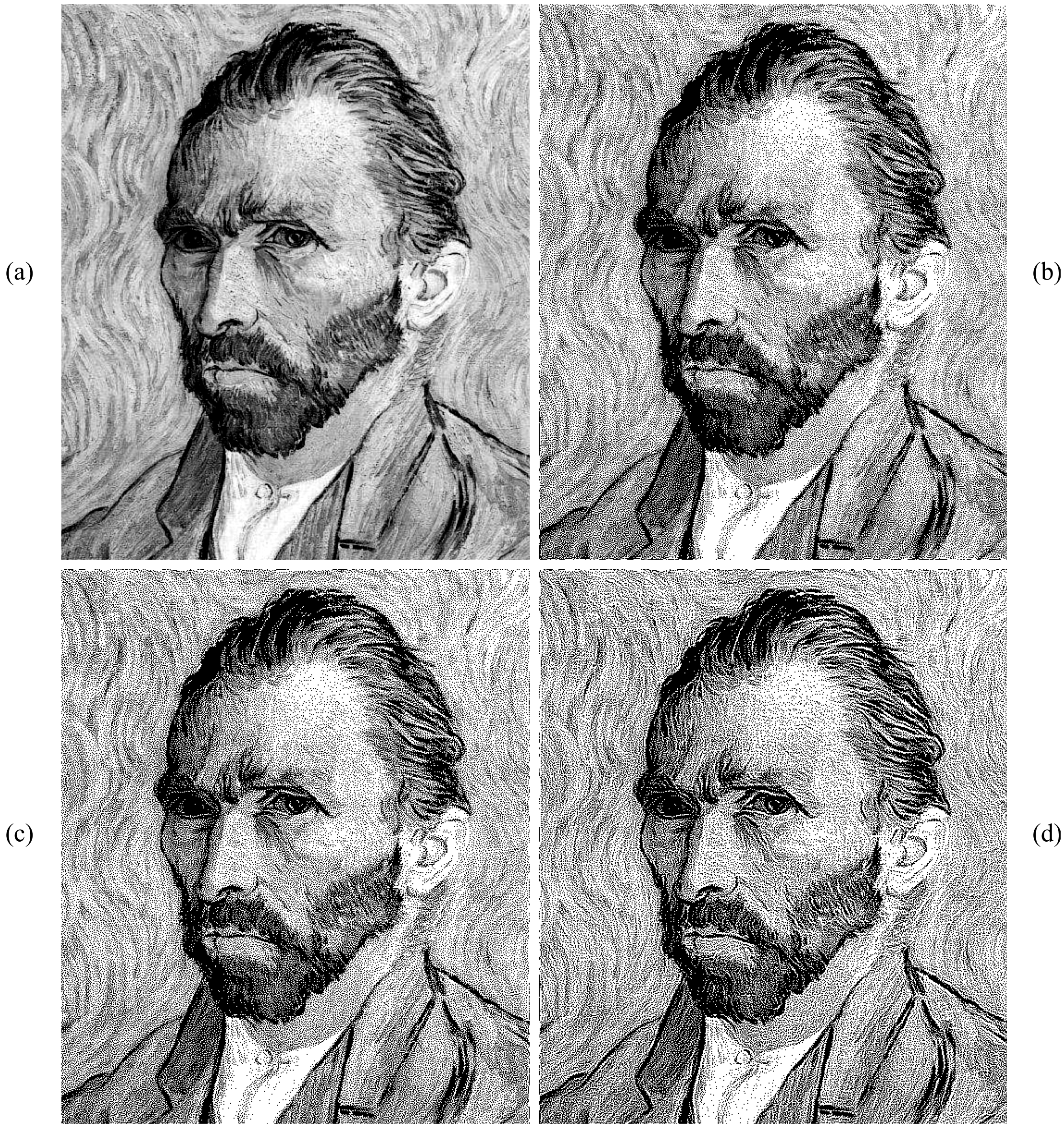

Figure 3. (a) Original grayscale image of *Portrait*. (b) Halftone image by classical IMCDP. (c) Halftone image by the proposed line-based IMCDP, $k_1 = 1$, $k_2 = 1.2$. (d) Halftone image by the proposed line-based IMCDP, $k_1 = 1$, $k_2 = 1.6$. Halftone images are displayed at resolution 200 dpi. This figure is best viewed in the electronic version of this paper.

Table II. Structural similarity evaluation according to MSSIM.

Image		Girl	Flower	Relief	Portrait	Road	Cat	Mole	Lion
Classical IMCDP		0.6328	0.6529	0.6535	0.6080	0.6278	0.6172	0.6248	0.5436
Line-based IMCDP	$k_1 = 1, k_2 = 1.2$	0.6493	0.6624	0.6682	0.6247	0.6460	0.6336	***0.6344***	0.5601
	$k_1 = 1, k_2 = 1.4$	0.6571	***0.6654***	0.6785	0.6361	0.6591	0.6479	0.6331	0.5726
	$k_1 = 1, k_2 = 1.6$	***0.6601***	0.6639	0.6869	0.6441	0.6682	0.6600	0.6297	0.5840
	$k_1 = 1, k_2 = 1.8$	0.6585	0.6575	0.6901	0.6486	0.6790	0.6687	0.6188	0.5914
	$k_1 = 1, k_2 = 2$	0.6555	0.6511	***0.6922***	***0.6487***	0.6860	***0.6762***	0.6115	***0.5935***
	$k_1 = 1, k_2 = 2.2$	0.6469	0.6417	0.6912	0.6470	***0.6906***	*0.6749*	0.5984	0.5916

Figure 4. Cropped region of the halftoned images in Fig. 3. (a) Classical IMCDP. (b) The proposed line-based IMCDP, $k_1 = 1$, $k_2 = 1.2$. (c) The proposed line-based IMCDP, $k_1 = 1$, $k_2 = 1.6$. Halftone images are displayed at resolution 100 dpi. This figure is best viewed in the electronic version of this paper.

Table III. Tone similarity evaluation according to MSE.

Image		Girl	Flower	Relief	Portrait	Road	Cat	Mole	Lion
Classical IMCDP		16.12	17.23	61.90	54.81	65.02	26.27	19.18	13.91
Line-based IMCDP	$k_1 = 1, k_2 = 1.2$	15.22	16.19	58.72	51.43	63.07	24.84	18.01	12.61
	$k_1 = 1, k_2 = 1.4$	14.63	15.67	56.44	49.29	60.80	***24.32***	17.30	11.70
	$k_1 = 1, k_2 = 1.6$	***14.50***	***15.61***	55.27	48.25	59.76	24.51	***17.10***	11.12
	$k_1 = 1, k_2 = 1.8$	14.83	16.13	***55.14***	***48.05***	***59.56***	25.49	17.75	***10.92***
	$k_1 = 1, k_2 = 2$	15.61	17.04	55.92	49.16	60.34	27.18	18.86	11.31
	$k_1 = 1, k_2 = 2.2$	16.91	18.73	57.68	50.72	62.03	29.78	20.74	12.16

k_2 is set to 1.6 or 1.8. Studying the results for MSSIM value shows that finding one single choice for k_2, which results in the best structural similarity for all the images, is more challenging. However, according to Fig. 5(b), $k_2 = 1.8$ results in an acceptable improvement in MSSIM.

According to the presented results, the moderate sharpness enhancement improves detail reproduction, and, at the same time, it increases resemblance to the original image. Therefore, by setting $k_1 = 1$ and $k_2 = 1.8$ the halftone output achieves a desirable degree of enhancement in sharpness and simultaneously improves the preservation of tonal and structural similarity for the proposed method.

Table IV summarizes the results of objective quality evaluation metrics (i.e., blur metric, MSSIM, and MSE) for both line-based IMCDP (with $k_1 = 1$, $k_2 = 1.8$) and classical IMCDP. Line-based IMCDP gives a lower blur metric, which indicates that halftone images reproduced by the line-based IMCDP are sharper than those reproduced by the classical IMCDP. More precisely, according to the sharpness metric, the line-based IMCDP generates halftones that are, on average, 28% sharper than images halftoned by classical IMCDP. Moreover, according to Table IV, the proposed method performs better than the classical IMCDP in preserving the structural and tonal similarity.

To have a visual example of the performance of the proposed method, the results for three of the test images are shown in Figure 6. Images displayed in this figure are processed by the contrast sensitivity model, as described in Section 3.4.1. It can be seen that the halftones created by the line-based IMCDP are perceived sharper; and the proposed method performs better than the classical IMCDP in preserving visually sensitive structure details, as well as the local tone. For instance, the structure of the wrinkles on the forehead, under the eye, and the hair in *Portrait* is better reproduced in Fig. 6(c) than in Fig. 6(a).

Comparing the results for the *Relief* image, in Figs. 6(a) and 6(c), reveals that our proposed halftoning algorithm also performs better than the classical IMCDP in displaying the highly-detailed appearance and conveying the feeling of the underlying 2.5D structural features of the sculpted relief.

Figure 7 shows the results for the *Cat* and *Lion*, which are natural photographs. As can be seen, the images in Fig. 7(c)

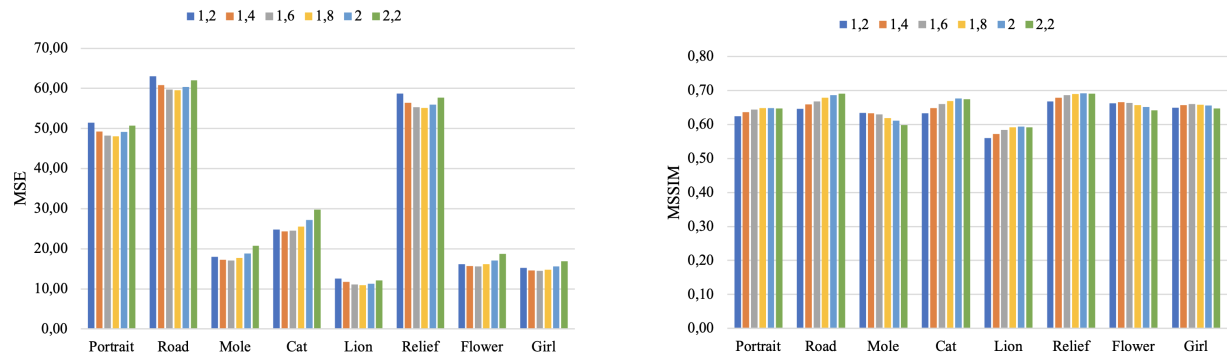

(a) (b)

Figure 5. Comparing (a) MSE (b) MSSIM for different ratios of k_2/k_1. The number associated with each bar's color corresponds to the ratio k_2/k_1. For instance, bars in green indicate the MSE and MSSIM value when k_1 and k_2 are set to 1 and 2.2, respectively.

Table IV. Comparison between the classical IMCDP and line-based IMCDP (with $k_1 = 1$, $k_2 = 1.8$).

	Image	Girl	Flower	Relief	Portrait	Road	Cat	Mole	Lion
Sharpness	Original image	0.2578	0.2622	0.1953	0.1862	0.1848	0.2086	0.2669	0.3267
	Classical IMCDP	0.3752	0.4252	0.4415	0.4056	0.3781	0.3731	0.3965	0.3710
	Line-based IMCDP	0.3158	0.3512	0.3598	0.3378	0.3192	0.3081	0.3296	0.3390
MSSIM	Classical IMCDP	0.6328	0.6529	0.6535	0.6080	0.6278	0.6172	0.6248	0.5436
	Line-based IMCDP	0.6585	0.6575	0.6901	0.6486	0.6790	0.6687	0.6188	0.5914
MSE	Classical IMCDP	16.12	17.23	61.90	54.81	65.02	26.27	19.18	13.91
	Line-based IMCDP	14.83	16.13	55.14	48.05	59.56	25.49	17.75	10.92

are sharper than those in Fig. 7(a). The detail reproduction of the hair and the direction of each single hair on the head of the cat and lion is better resolved in Fig. 7(c). Images halftoned by the proposed line-based IMCDP are percieved more realistic than the classical IMCDP. According to Figs. 6 and 7, the proposed algorithm performs well on different types of images, however, the effect is better illustrated in structured regions in an image. Visual comparison of the outputs of the two halftoning algorithms displayed in Figs. 6 and 7 clearly verifies the results provided in Table IV.

4.2 *Subjective Evaluation Results*

To verify the objective evaluation, we conduct a subjective experiment. Figure 8 illustrates the results of the subjective experiment for 10 observers. According to Fig. 8(a), increasing the ratio k_2/k_1 makes the difference between the line-based IMCDP and the classical IMCDP more perceptible.

For small values of k_2/k_1, observers find it more difficult to perceive the difference between different halftoning algorithms than for large values of k_2/k_1. Fig. 8(b) shows that as k_2 increases, the preference for the proposed line-based IMCDP over the classical IMCDP grows.

According to the participants, 47% of the images being halftoned by the line-based IMCDP with $k_2 = 1.4$ better resemble the details of the original image than the classical IMCDP. The preference increases to 81% as k_2 reaches 1.8. Fig. 8(c) presents the percentage of responses, which prefer the classical IMCDP over the line-based IMCDP. As can be seen at $k_2 = 1.6$ and $k_2 = 1.8$, only 9% of the responses vote for the classical IMCDP, which verifies that selecting $k_2 = 1.8$, based on the objective evaluation metrics, is a suitable value for k_2.

Moreover, it is important to notice the increase of preference for the classical IMCDP for large values for k_2 (i.e., at 2 and 2.2) in Fig. 8(c). According to the observers' responses, for values of k_2 larger than 1.8, the percentage of selecting the classical IMCDP increases. Moreover, according to Fig. 8(b), it reveals that the preference for the line-based IMCDP for values of k_2 larger than 1.8 grows at a low rate. This can be attributed to unwanted structures, which appear in the images for large values of k_2. Figure 9 illustrates two trials for the images *Girl* and *Flower*. The original continuous-tone image is placed in the middle, the image to the left is halftoned by the classical IMCDP, and the image to the right is halftoned by the line-based IMCDP with $k_2 = 2.2$. It seems that the observers could not perceive

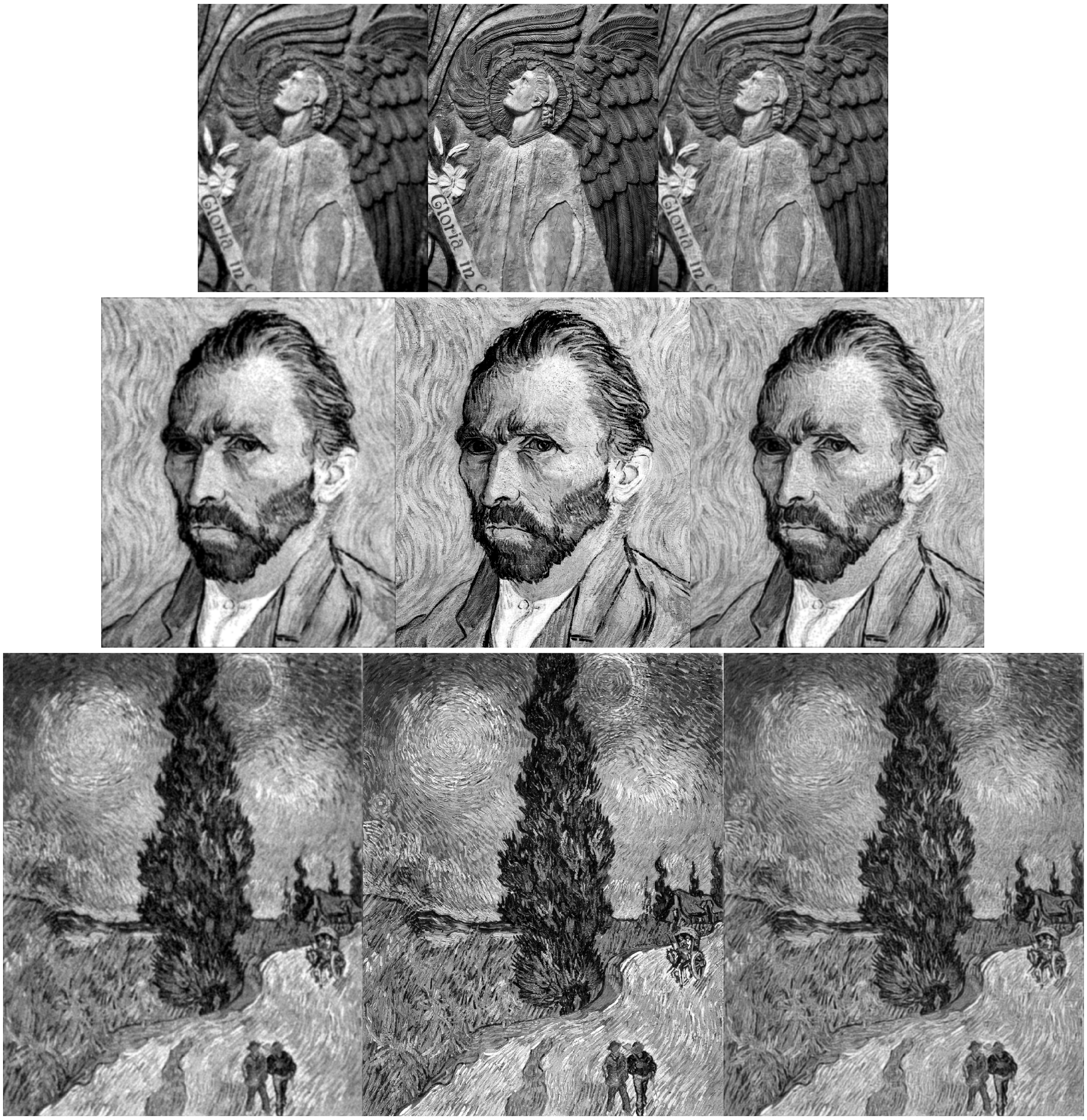

(a) (b) (c)

Figure 6. Results comparison for *Relief* (first row), *Portrait* (second row), and *Road* (third row) images. (a) Classical IMCDP (b) original image (c) line-based IMCDP (with $k_1 = 1$, $k_2 = 1.8$). Images are processed by the human perceptual model, as described in Section 3.4.1.

the extra unwanted structures in some of the images due to their distribution in the image. For example, in Fig. 9(a), the extra unwanted structures are not clearly visible, however, in Fig. 9(b), the unwanted structures in the background and the flower may have been noticeable to the observers. This means that the distribution of the extra unwanted structures, added at large values of k_2, may have influenced the observers' responses. Hence, for some images with $k_2 = 2$ and 2.2, the observers select the classical IMCDP over the line-based IMCDP in terms of structural resemblance to the original image.

4.3 *Computation Time*

Iterative halftoning algorithms are usually computationally expensive. In this work, as the line detection task is done during the pre-processing step, the proposed line-based IMCDP is as fast as the classical IMCDP. The computation time depends on the size of the image. For a 600×500 image, the required time to perform the pre-processing step is an average time of 600 s (2 msec per pixel), and the halftoning step generates the structure-based halftone result by running 191,550 iterations in an average time of 5 s (24.8 μs per iteration). The reported timing is based on the

(a) (b) (c)

Figure 7. Results comparison for *Cat* (first row) and *Lion* (second row) images. (a) Classical IMCDP (b) original image (c) line-based IMCDP (with $k_1 = 1$, $k_2 = 1.8$). Images are processed by the human perceptual model, as described in Section 3.4.1.

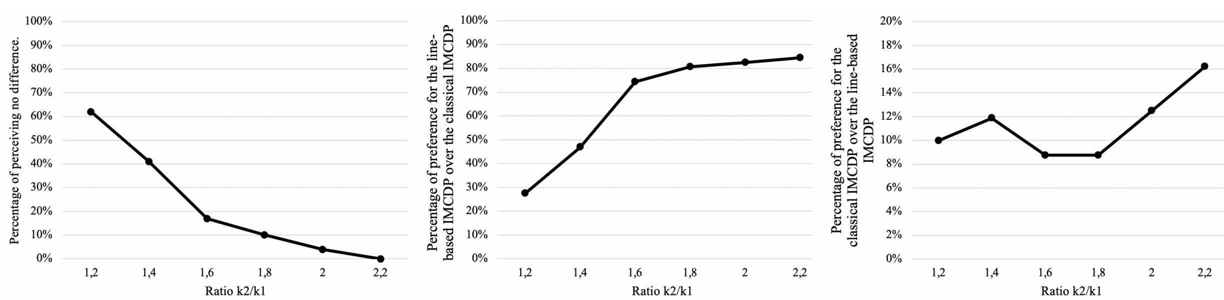

(a) (b) (c)

Figure 8. Subjective evaluation results for 10 observers. (a) Percentage of perceiving no difference (b) percentage of preference for the proposed line-based IMCDP over the classical IMCDP (c) percentage of preference for the classical IMCDP over the proposed line-based IMCDP. (On the horizontal axis, the ratio varies by setting $k_1 = 1$ and increasing k_2 from 1.2 to 2.2.)

current implementation of the proposed algorithm in Matlab on a MacBook Pro equipped with 2.6 GHz Intel Core i7 CPU and 16 GB 2400 MHz DDR4 memory.

4.4 *Discussion*

The aim of this study was to develop a halftoning algorithm that better preserves edges while increasing the tonal and structural similarity. Sharpening the input image prior to halftoning could obviously increase the sharpness of the output halftone, but it is not the best solution to create halftones with a sharpness closer to the original image. Sharpening an image before halftoning manipulates the original information of the input image. This paper presented an algorithm that generates sharper halftones through the halftoning process without changing the original input image. In addition, it simultaneously improves the resemblance to the original image.

The classical IMCDP has been extended to the 3D domain and thoroughly discussed in Ref. [34]. Moreover, It was shown that applying different halftones according to the geometrical characteristics of the 3D surface affects the perceived 3D structures of a 3D printed shape [24, 35]; that means halftoning could control the visual quality of 3D printed surfaces. As the merit of the proposed algorithm is

(a)

(b)

Figure 9. Examples of two trials for images (a) *Girl* and (b) *Flower*. The original continuous-tone image is placed in the middle, the image to the left is halftoned by the classical IMCDP, and the image to the right is halftoned by the line-based IMCDP with $k_2 = 2.2$.

to increase the sharpness through the halftoning process, it makes it feasible to consider both the structure of the image being mapped on a 3D surface and the underlying 3D geometrical surface structures while applying the different halftones.

The proposed line-based IMCDP method could be extended to halftone 3D surfaces. In the 3D extension of the algorithm, different halftone structures could be adapted to different parts of the 3D printed object by benefiting both the content of the images being mapped and the 3D geometrical structure of the underlying printed surface. We believe that adjusting the degree of sharpness enhancement could be employed to compensate for the loss of the features caused by the 3D manufacturing process. Achieving this goal requires a structure-aware sharpening effect that occurs adaptively through halftoning, which is clearly beyond sharpening the input image prior to halftoning.

5. CONCLUSION AND FUTURE WORK

In this paper, we presented a line-based IMCDP halftoning algorithm that aligns the halftone structure with regard to the image content. Compared to the classical IMCDP, the proposed algorithm improves the representation of the image structure by enhancing the sharpness, and, therefore, it could better display the feeling of the underlying 2.5D structural features. Our study revealed that a moderate degree of sharpness enhancement simultaneously results in higher structural similarity and tone consistency. The objective evaluation results have been verified through subjective assessment. Both indicated that the proposed algorithm is superior to the classical version in preserving image structure and fine details.

For future work, we plan to extend the line-based IMCDP to the 3D domain and develop an adaptive structure-aware 3D halftoning algorithm. The algorithm could adaptively adjust the degree of sharpness enhancement (ratio k_2/k_1) and the angle of the line halftones according to the image content, as well as the geometrical spatial information of the shape during the halftoning process without changing the input image. We believe that further studies in this direction may help to gain new insight into the impact of halftoning in improving the visual quality of surface reproduction.

ACKNOWLEDGMENT

This project was funded by ApPEARS (Appearance Printing European Advanced Research School), the European Union's Horizon 2020 programme under the Marie Skłodowska-Curie grant agreement No. 814158.

REFERENCES

1 R. Ulichney, *Digital Halftoning* (MIT Press, Cambridge, MA, 1987).

2 R. W. Floyd and L. Steinberg, "An adaptive algorithm for spatial grayscale," Proc. Soc. Inf. Disp. **17**, 75–77 (1976).

3 V. Ostromoukhov, "A simple and efficient error-diffusion algorithm," *Proc. 28th Annual Conf. on Computer Graphics and Interactive Techniques* (ACM, New York City, NY, 2001), pp. 567–572.

4. B. Zhou and X. Fang, "Improving mid-tone quality of variable-coefficient error diffusion using threshold modulation," ACM Trans. Graph. **22**, 437–444 (2003).
5. J. F. Jarvis, C.N. Judice, and W. H. Ninke, "A survey of techniques for the display of continuous tone pictures on bilevel displays," Comput. Graph. Image Process. **5**, 13–40 (1976).
6. P. Stucki, "MECCA-A multiple-error correction computation algorithm for Bi-level image hardcopy reproduction," *IBM Thomas J. Watson Research Division*. Published online (1981).
7. M. Analoui and J. P. Allebach, "Model-based halftoning using direct binary search," Proc. SPIE **1666** (1992).
8. S. Gooran, "Dependent color halftoning: Better quality with less ink," J. Imaging Sci. Technol. **48**, 354–362 (2004).
9. D. J. Lieberman and J. P. Allebach, "Efficient model based halftoning using direct binary search," *Proc. Int'l. Conf. on Image Processing* (IEEE, Piscataway, NJ, 1997), 1, pp. 775–778.
10. D. J. Lieberman and J. P. Allebach., "A dual interpretation for direct binary search and its implications for tone reproduction and texture quality," IEEE Trans. Image Process. **9**, 1950–1963 (2000).
11. H. Li and D. Mould, "Contrast-aware halftoning," Comput. Graph. Forum **29**, 273–280 (2010).
12. R. Eschbach and K. T. Knox, "Error-diffusion algorithm with edge enhancement," J. Opt. Soc. Am. A **8**, 1844–1850 (1991).
13. W. M. Pang, Y. Qu, T. T. Wong, D. Cohen-Or, and P. A. Heng, "Structure-aware halftoning," *ACM SIGGRAPH 2008 Papers* (ACM, New York City, NY, 2008), pp. 1–8.
14. J. Chang, B. Alain, and V. Ostromoukhov, "Structure-aware error diffusion," ACM Trans. Graph. **28**, 1–8 (2009).
15. L. Liu, W. Chen, W. Zheng, and W. Geng, "Structure-aware error-diffusion approach using entropy-constrained threshold modulation," Vis. Comput. **30**, 1145–1156 (2014).
16. D. Li, T. Kiyotomo, T. Horiuchi, M. Tanaka, and K. Shigeta, "Texture-aware error diffusion algorithm for multi-level digital halftoning," J. Imaging Sci. Technol. **64**, 50410-1 (2020).
17. N. J. Kwak, S.P. Ryu, and J. H. Ahn, "Edge-enhanced error diffusion halftoning using human visual properties," *Int'l. Conf. on Hybrid Information Technology* (IEEE, Piscataway, NJ, 2006), 1, pp. 499–504.
18. X. Li, "Edge-directed error diffusion halftoning," IEEE Signal Process. Lett. **13**, 688–690 (2006).
19. H. S. Lee, K.K. Kong, and K. S. Hong, "Laplacian based structure-aware error diffusion," *IEEE Int'l. Conf. on Image Processing* (IEEE, Piscataway, NJ, 2010), pp. 525–528.
20. P. V. C. Hough, Method and means for recognizing complex patterns," Published online December 18, US Patent 3,069,654, (1962).
21. P. Li and J. P. Allebach, "Tone-dependent error diffusion," IEEE Trans. Image Process. **13**, 201–215 (2004).
22. F. A. Baqai and J. P. Allebach, "Halftoning via direct binary search using analytical and stochastic printer models," IEEE Trans. Image Process. **12**, 1–15 (2003).
23. S. Gooran and B. Kruse, "High-speed first- and second-order frequency modulated halftoning," J. Electron. Imaging **24**, 1–19 (2015).
24. S. Gooran and F. Abedini, "3D surface structures and 3D halftoning," *Proc. IS&T Printing for Fabrication 2020* (IS&T, Springfield, 2020), 2020, pp. 75–80.
25. J. Canny, "A computational approach to edge detection," IEEE Trans. Pattern Anal. Mach. Intell. **PAMI-8**, 679–698 (1986).
26. T. N. Pappas and D. L. Neuhoff, "Least-squares model-based halftoning," IEEE Trans. Image Process. **8**, 1102–1116 (1999).
27. R. Näsänen, "Visibility of halftone dot textures," IEEE Trans. Syst. Man Cybern. 920–924 (1984).
28. S. J. Daly, M. Rabbani, and C. T. Chen, "Digital image compression and transmission system visually weighted transform coefficients," Published online October 25, US Patent 4,780,761 (1988).
29. F. Crete, T. Dolmiere, P. Ladret, and M. Nicolas, "The blur effect: perception and estimation with a new no-reference perceptual blur metric," Proc. SPIE **6492**, 649201 (2007).
30. Z. Wang, A.C. Bovik, H.R. Sheikh, and E.P. Simoncelli, "Image quality assessment: from error visibility to structural similarity," IEEE Trans. Image Process. **13**, 600–612 (2004).
31. M. Grimes, "Subway Girl, oil painting" This image was marked with a CC BY-NC-ND 2.0 license. Accessed June 21, (2021). https://search.creativecommons.org/photos/e5437db9-091b-49ad-9804-ed33e05fdf52.
32. M. Streepy, "*Flower 2*, oil painting" This image was marked with a CC BY-NC-ND 2.0 license. Accessed June 21, (2021). https://search.creativecommons.org/photos/ebdb4c0d-089c-49ca-91f8-0ec6e3ec1151.
33. Kotomi, "Relief for the Chapel," This image was marked with a CC BY-NC 2.0 license. Accessed June 21, (2021). https://search.creativecommons.org/photos/54599a45-885f-4760-891e-142d23503b05.
34. F. Abedini, S. Gooran, and D. Nystrm, "3D halftoning based on iterative method controlling dot placement," *Proc. IS&T Printing for Fabrication 2020* (IS&T, Springfield, 2020), 2020, pp. 69–74.
35. F. Abedini, S. Gooran, and D. Nystrm, "The effect of halftoning on the appearance of 3D printed surfaces," *47th Annual Conf. of Iarigai* (Iarigai, Darmstadt, Germany, 2021).